Promoted Reduction of Tellurite and Formation of Extracellular Tellurium Nanorods by Concerted Reaction between Iron and Shewanella oneidensis MR-1

ARTICLE *in* ENVIRONMENTAL SCIENCE & TECHNOLOGY · JUNE 2013

Impact Factor: 5.33 · DOI: 10.1021/es401302w · Source: PubMed

5 AUTHORS, INCLUDING:

Dong-Hun Kim
Korean Institute of Geoscience and Mineral Re…
8 PUBLICATIONS **49** CITATIONS
SEE PROFILE

Min Gyu Kim
Pohang University of Science and Technology
151 PUBLICATIONS **5,116** CITATIONS
SEE PROFILE

Shenghua Jiang
Shanghai Taijing Investment Group Co. Ltd., C…
14 PUBLICATIONS **100** CITATIONS
SEE PROFILE

Ji-Hoon Lee
Chonbuk National University
29 PUBLICATIONS **425** CITATIONS
SEE PROFILE

Environmental Science & Technology

Article

pubs.acs.org/est

Promoted Reduction of Tellurite and Formation of Extracellular Tellurium Nanorods by Concerted Reaction between Iron and *Shewanella oneidensis* MR-1

Dong-Hun Kim,[†] Min-Gyu Kim,[‡] Shenghua Jiang,[§] Ji-Hoon Lee,[∥] and Hor-Gil Hur*[,†]

[†]School of Environmental Science and Engineering, Gwangju Institute of Science and Technology, Gwangju 500-712, Republic of Korea

[‡]Pohang Accelerator Laboratory, Beamline Research, Pohang 790-784, Republic of Korea

[§]Department of Civil and Environmental Engineering, Stanford University, Stanford, California 94305, United States

[∥]Geologic Environmental Division, Groundwater Department, Korea Institute of Geoscience and Mineral Resources, Daejeon 305-350, Republic of Korea

Supporting Information

ABSTRACT: The reduction of tellurite (Te(IV)) by dissimilatory metal reducing bacterium, *Shewanella oneidensis* MR-1, was promoted in the presence of Fe(III) in comparison with Te(IV) bioreduction in the absence of Fe(III). Electron microscopic analyses revealed that iron promoted Te(IV) reduction led to form exclusively extracellular crystalline Te(0) nanorods, as compared to the mostly intracellular formation of Te(0) nanorods in the absence of Fe(III). The Te K-edge X-ray absorption spectrometric analyses demonstrated that *S. oneidensis* MR-1 in the presence of Fe(III) reduced Te(IV) to less harmful metallic Te(0) nanorods through the precipitation of tellurite ($Te(IV)O_x$) complex by the bacterial respiration of Fe(III) to Fe(II) under anaerobic conditions. However, Fe(II) ion itself was only able to precipitate the solid tellurite ($Te(IV)O_x$) complex from the Te(IV) solution, which was not further reduced to Te(0). The results clearly indicated that bacterial *S. oneidensis* MR-1 plays important roles in the reduction and crystallization of Te(0) nanorods by as yet undetermined biochemical mechanisms. As compared to the slow bacterial Te(IV) reduction in the absence of Fe(III), the rapid reduction of Te(IV) to Te(0) by the concerted biogeochemical reaction between Fe(II) and *S. oneidensis* MR-1 could be applied for the sequestration and detoxification of Te(IV) in the environments as well as for the preparation of extracellular Te(0) nanorod structures.

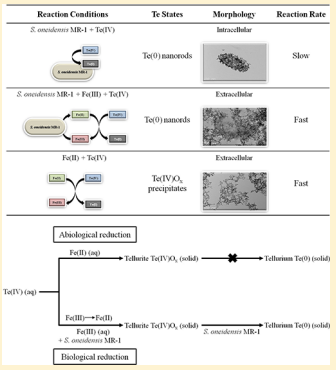

INTRODUCTION

Tellurium (Te) and its compounds are widely used in petroleum refining, the electronic and photoelectronic industries, optics, glass, and sensors.[1−4] However, as expected, the recent expanded use of Te leads to the environmental contamination.[5] In the environment, soluble oxyanions tellurite (TeO_3^{2-}, Te(IV)) is highly toxic to both eukaryotic and prokaryotic cells at a concentration as low as 1 μg/mL.[5,6] The redox chemistry of Te is crucial in governing its mobility and toxicity. The elemental state of Te(0) is insoluble in water and has low bioavailability and toxicity. Therefore, the reduction of Te(IV) to insoluble and less toxic Te(0) is an effective strategy for relieving the high toxicity of Te(IV) in the environments.[4,6] Several recent studies have shown that Te can be removed from aqueous solution via the reduction of Te(IV) to insoluble and low toxic forms.[3,4,6−10] Microbial processes can contribute to Te(IV) reduction by direct enzymatic reduction,[5,7,10] or through indirect redox active organic molecules, such as quinines.[4] However, the geochemical significance of this mechanism is not fully understood.[5,6]

The biogeochemical cycles of major and trace elements in the environments are driven by redox processes, which also affect the chemical speciation, bioavailability, toxicity, and mobility of the elements. Especially, the most abundant iron ion on the Earth's surface plays a particularly important role in environmental biogeochemistry. In fact, the soluble Fe(II) by reduction of iron oxide and Fe-bearing minerals by various biogeochemical reactions can act as powerful reducing agents in a variety of abiotic redox processes[11−16] and can be implicated in the processes for removing the heavy metals or contaminants.[12,14,16−19]

Dissimilatory metal reducing bacterium, *Shewanella oneidensis* MR-1, is recognized for its broad spectrum of involvements within the geochemical cycles of key elements by coupling the reduction of insoluble metal oxides to the oxidation of the organic carbon under anaerobic conditions.[20−24] In addition to biological reduction of Fe(III), U(VI), Se(IV), etc., by *S. oneidensis* MR-1, recent studies have shown that the strain MR-1 can reduce Te(IV) using as a final electron acceptor under

Received: March 25, 2013
Revised: June 8, 2013
Accepted: June 26, 2013
Published: June 26, 2013

the anaerobic condition with mostly forming intracellular Te(0) nanorods.[9,25]

Here, we demonstrate the iron-mediated enhanced Te(IV) reduction via two steps of closely coupled biological and/or abiological reaction pathways under anaerobic conditions, which could be used for sequestration and removal of toxic Te(IV) in the environments as well as for the preparation of the well characterized Te(0) nanorod structures outside of cells through environmentally friendly processes.

MATERIALS AND METHODS

Chemicals, Bacterial Strains and Culture Conditions. All chemicals and reagents were purchased from Sigma-Aldrich (St. Louis, MO) and Fisher Scientific (Pittsburgh, PA). The facultative anaerobic bacterium *S. oneidensis* MR-1 was grown aerobically on Luria−Bertani (LB) broth at 30 °C with shaking at 200 rpm for 12 h. Cells were centrifuged (9000 *g* for 10 min), washed with sterile HEPES buffer (10 mM, pH 7.0), and resuspended in HEPES buffer. Cells were subsequently inoculated into serum bottles to achieve an optical density (OD) of 0.1 at a wavelength of 600 nm of the total volume of sterilized HEPES-buffered basal medium,[26] which contained 10 mM sodium lactate (0.22 μm filter sterilized) as an electron donor and other chemicals were added according to the reaction conditions. To evaluate the effect of diverse reducing agents on Te(IV) reduction, 10 mM each of Fe(III)-citrate, akaganeite,[27,28] manganese oxide,[29] sodium thiosulfate, sodium fumarate, and sodium nitrate was added in HEPES-buffered basal medium which contains lactate, *S. oneidensis* MR-1, and 1 mM Te(IV) under anaerobic conditions. Direct reduction of Te(IV) by *S. oneidensis* MR-1 was tested with 10 mM lactate and 1 mM Te(IV) as an electron donor and acceptor, respectively. All incubations were performed in triplicate and carried out in the absence of light without agitation at 30 °C under anaerobic conditions.

Analytical Methods. The culture medium was periodically sampled during incubation to determine the concentration of Fe(II) and Te(IV) in solution phase. For each sample, 1 mL of culture medium was collected using sterile syringes at the selected time and then immediately passed through a 0.22 μm membrane filter (MFS-25, Advantec MFS, Inc., Dublin, CA). The concentration of Fe(II) was monitored spectrophotometrically at 562 nm using ferrozine assay.[30] To measure Te(IV) concentration, the aqueous phase was diluted with 2% (v/v) HNO_3 and analyzed by inductively coupled plasma-mass spectroscopy (ICP-MS, 7500ce, Agilent Technology, Palo Alto, CA). All measurements were conducted in triplicate. The mineralogical property of the nanostructures was analyzed using powder X-ray diffraction (XRD, D/MAX Uitima III, Rigaku, Tokyo, Japan) equipped with monochromatic high-intensity Cu Kα radiation (λ = 1.54056 Å).

Electron Microscopic Analyses. The formation and accumulation of tellurium nanostructures in the bacterial culture medium were periodically determined by SEM and TEM analyses during reaction period. Samples were collected at a selected time and centrifuged at 9000 *g* for 5 min. The pellets were washed three times and resuspended with deionized water, and dropped onto a silica wafer for SEM imaging, which was operated at 10 kV (SEM, XL30-FEG, Philips, Eindhoven, Netherlands). For TEM imaging, washed cells were placed onto carbon-coated 200-mesh copper grids. The images of whole mounts were obtained at 200 kV using a JEOL JEM-2100 high resolution TEM (JEOL, Tokyo, Japan).

Te K-Edge X-ray Absorption Spectroscopy. Te K-edge X-ray absorption spectra, X-ray absorption near edge structure (XANES) and extended X-ray absorption fine structure (EXAFS), were collected on the BL10C beamline at the Pohang light source (PLS-II) with a ring current of 100 mA at 3.0 GeV. The monochromatic X-ray beam could be obtained from high intense X-ray photons of multipole wiggler source using liquid-nitrogen cooled Si (111) double crystal monochromator (Bruker ASC). The X-ray absorption spectroscopic data were recorded for the uniformly dispersed powder samples with a proper thickness on the polyimide film, in transmission mode with N_2 gas-filled ionization chambers as detectors. All samples were maintained in an Ar atmosphere before the XAFS measurement in order to remove any air-borne contamination leading to sample oxidation. Higher order harmonic contaminations were eliminated by detuning to reduce the incident X-ray intensity by ∼20%. Energy calibration has been simultaneously carried out for each measurement with reference Te metal powder placed in front of the third ion chamber. The data reductions of the experimental spectra to normalized XANES and Fourier-transformed radial distribution function (RDF) were performed through the standard XAFS procedure.

RESULTS AND DISCUSSION

Effect of Diverse Reducing Agents on Te(IV) Reduction in the Culture of *S. oneidensis* MR-1. It has been known that dissimilatory metal reducing bacterium, *S. oneidensis* MR-1, can reduce Te(IV) directly using organic compounds as electron donors.[9,25] In our previous study,[25] *S. oneidensis* MR-1 slowly reduced Te(IV) to elemental tellurium Te(0) in which 90% of the initial concentration of Te(IV) at 0.1 mM was reduced in 5 days incubation, followed by the intracellular accumulation of needle shaped crystalline Te(0) nanorods. In this study, we examined the effect of diverse reducing agents, Fe(III)-citrate, akaganeite, manganese oxide, sodium thiosulfate, sodium fumarate, and sodium nitrate, as an electron shuttle on the reduction of Te(IV) in the anaerobic culture of *S. oneidensis* MR-1. In Table 1, the reduction rate of Te(IV) by *S. oneidensis* MR-1 was significantly increased when akaganeite, Fe(III)-citrate, and manganese oxide were added to the bacterial culture than when *S. oneidensis* MR-1 alone was added. The initial concentration of Te(IV) at 1 mM was reduced up to 99%, 94%, and 76% within 24 h in the bacterial culture of *S. oneidensis* MR-1 containing akaganeite, Fe(III)-citrate, and manganese oxide, respectively. The higher reduction of Te(IV) by *S. oneidensis* MR-1 with akaganeite

Table 1. Effect of Diverse Reducing Agents on the Reduction of Te(IV) in the Presence of *S. oneidensis* MR-1

reactions	concentration of Te(IV) remained in the aqueous phase at 24 h incubation (mM)
Control (culture medium alone)	0.97 ± 0.03
S. oneidensis MR-1 alone	0.85 ± 0.03
S. oneidensis MR-1 + Fe(III)-citrate	0.06 ± 0.01
S. oneidensis MR-1 + akaganeite	0.02 ± 0.01
S. oneidensis MR-1 + manganese oxide	0.49 ± 0.13
S. oneidensis MR-1 + thiosulfate	0.84 ± 0.06
S. oneidensis MR-1 + fumarate	0.78 ± 0.05
S. oneidensis MR-1 + nitrate	0.96 ± 0.04

dx.doi.org/10.1021/es401302w | *Environ. Sci. Technol.* 2013, 47, 8709−8715

than that by strain MR-1with Fe(III)-citrate could be attribute to adsorption of Te(IV) ion onto the insoluble akaganeite structure as suggested within previous reports.[31−34] In contrast, Te(IV) was reduced by 16%, 22%, and 10% using a culture of *S. oneidensis* MR-1 with thiosulfate, fumarate, and nitrate, respectively, in 24 h incubation, indicating addition of Fe(III) to the culture of *S. oneidensis* MR-1, which stimulated the reduction of Te(IV).

Effects of Fe(III) and Fe(II) on Te(IV) Reduction in the Culture of *S. oneidensis* MR-1. To better understand the effects of iron on the Te(IV) reduction by *S. oneidensis* MR-1 under anaerobic conditions, Fe(III)-citrate was used for the further experiments. Figure 1a shows kinetics of Te(IV)

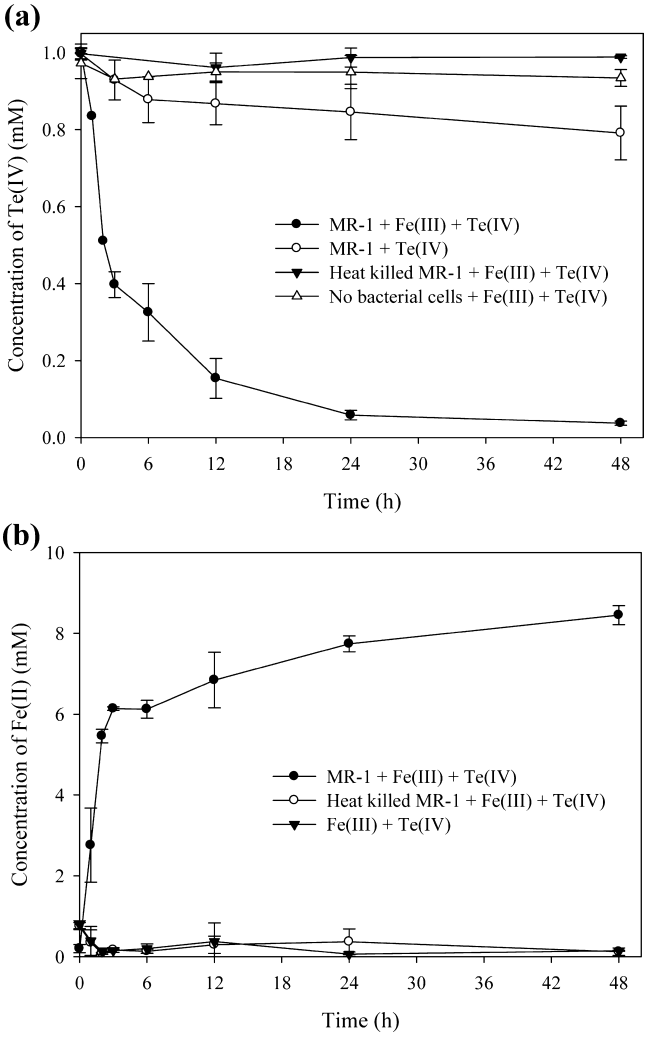

Figure 1. Kinetics of Te(IV) (a) and Fe(II) (b) in the aqueous phase of the various incubation conditions. *S. oneidensis* MR-1 was incubated with Fe(III) and Te(IV) together under anaerobic conditions.

reduction varies under different incubation conditions. *S. oneidensis* MR-1 in the presence of Fe(III) at 10 mM dramatically increased Te(IV) reduction up to the amount of 61.7% in 3 h incubation, as compared to the reaction conditions without either Fe(III) or *S. oneidensis* MR-1, which did not show Te(IV) reduction. Although the MR-1 culture in the absence of Fe(III) showed barely 10% Te(IV) reduction in 3 h incubation, no further significant reduction of Te(IV) occurred as incubation time passed. The lesser reduction of 1 mM Te(IV) is possibly due to physiological toxicity of Te(IV) to the strain.[5,7] In addition, the heat-killed *S. oneidensis* MR-1 with Fe(III) or Fe(III) alone did not show Te(IV) reduction. While monitoring the kinetics of Te(IV) reduction by *S. oneidensis* MR-1 in the presence of Fe(III) under anaerobic conditions, the oxidation state of iron (Fe(III) and Fe(II)) was also tracked (Figure 1b). The amount of Fe(II) in the culture medium of *S. oneidensis* MR-1 in the presence of Fe(III) and Te(IV) at each 10 mM and 1 mM, respectively, was increased with incubation period. *S. oneidensis* MR-1 rapidly produced Fe(II) at approximately 6 mM in 3 h incubation, and then maintained Fe(II) at 8.5 mM to the end of incubation. In contrast, controls containing Fe(III) with the heat-killed bacterial cells and Fe(III) alone did not produce Fe(II) and reduce Te(IV) to Te(0). These results suggested that reducing power for Te(IV) reduction could be supported chemically from Fe(II) produced by *S. oneidensis* MR-1. The Fe(III) concentration also has an affect on the Te(IV) reduction in the presence of *S. oneidensis* MR-1. Higher concentration of Fe(III) showed a greater rate of Te(IV) reduction than evident at low concentration of Fe(III) (Figure S1 of the Supporting Information, SI). In the presence of *S. oneidensis* MR-1, 10 mM of Fe(III) showed more than 94% reduction of Te(IV) while 1 mM and 0.1 mM of Fe(III) showed 76% and 29% of Te(IV) reduction, respectively, at 24 h incubation. There could be another possibility of the direct chemical reduction of Te(IV) by chemical reducing reagent such as Fe(II) ion. Previous studies report that the chemical reductants such as Fe(II) and dissolved sulfide in natural environments can accelerate reduction of Cr(VI),[14,15,19] Tc(VII),[17] and CCl_4.[18] To test the possibility for the chemical reduction of Te(IV) by Fe(II) in the absence of *S. oneidensis* MR-1, $FeCl_2$ at 10 mM in the final concentration was added to the solution containing Te(IV). Initial Te(IV) in medium containing the abiological Fe(II) rapidly decreased more than 97% in 1 h reaction (Figure 2). Similar results were also observed in the bacterial culture where biological Fe(II) was preformed by *S. oneidensis* MR-1 with Fe(III) for 24 h incubation. The bacterial culture with preformed biological Fe(II) reduced Te(IV) more than 95% of initial Te(IV) within 1 h reaction. In contrast, the Te(IV) reduction reaction was not

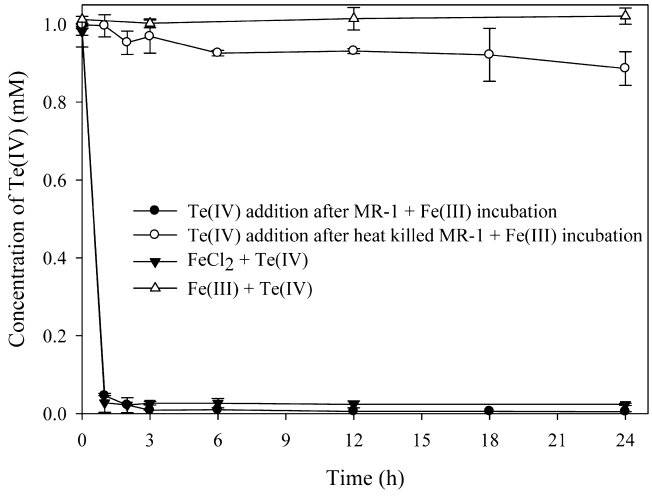

Figure 2. Kinetics of Te(IV) and Fe(II) in the aqueous phase of various incubation conditions. Active or heat-killed *S. oneidensis* MR-1 was preincubated with Fe(III) for 24 h and abiological Fe(II) and Fe(III) were prepared as $FeCl_2$ and Fe(III)-citrate.

dx.doi.org/10.1021/es401302w | *Environ. Sci. Technol.* 2013, 47, 8709−8715

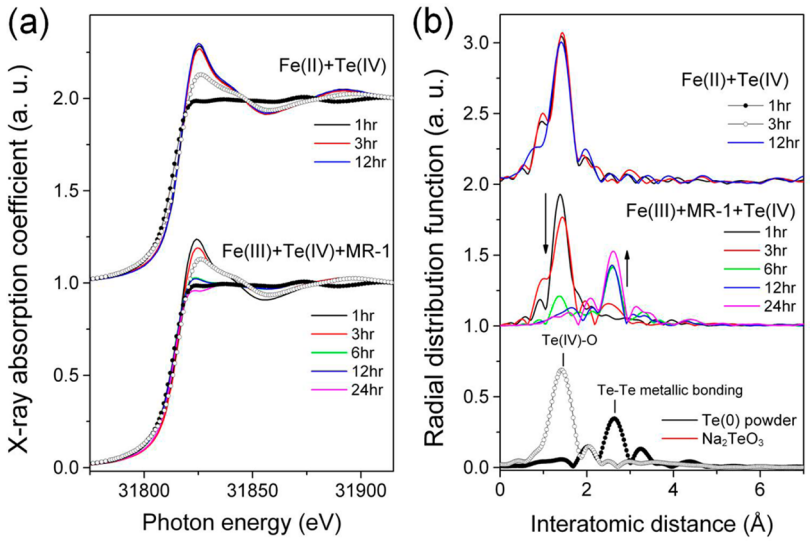

Figure 3. (a) Normalized Te K-edge X-ray absorption near edge structure (XANES) and (b) corresponding radial distribution function of k^2-weighted Te K-edge extended X-ray absorption fine structure (EXAFS) for both incubation time in biological reduction (Fe(III) + Te(IV) + *S. oneidensis* MR-1) and reaction time in abiological reduction (Fe(II) + Te(IV) + no bacterial inoculation). In each plot, metallic tellurium powder (Te(0), filled circle) and tellurite (Na_2TeO_3, open circle) have been compared.

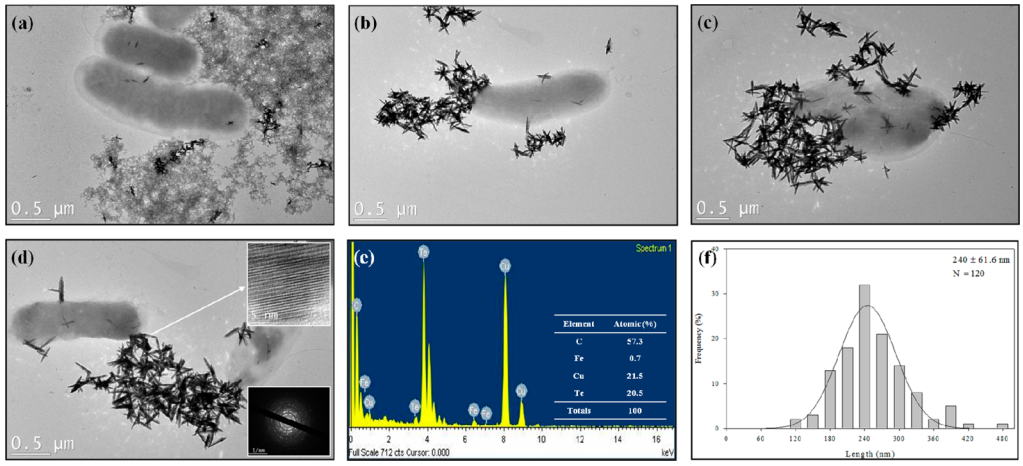

Figure 4. TEM images of (a) to (d) for extracellular Te(0) nanorods formed by concurrent incubation of Fe(III) with Te(IV) in the presence of *S. oneidensis* MR-1 with SAED pattern (d inserted), EDS spectra (e), and length distribution (f) at 24 h incubation. The TEM images of (a) to (d) were taken at 1, 3, 12, and 24 h incubation, respectively.

observed in the absence of Fe(II). It should be noted that the X-ray absorption spectroscopic study revealed the chemical reduction of Te(IV) by Fe(II) in the absence of *S. oneidensis* MR-1 was not able to proceed to total reduction to metallic Te(0) state, but was likely to precipitate in the form of tellurite ($Te(IV)O_x$) from the solution. This is supported by the normalized Te K-edge X-ray absorption near edge structure (XANES) and the corresponding radial distribution function of Fourier-transformed k^2-weighted Te K-edge extended X-ray absorption fine structure (EXAFS) for incubation time in both biological reduction (Fe(III) + Te(IV) + *S. oneidensis* MR-1) and chemical reduction (Fe(II) + Te(IV)) (Figure 3). As shown in Figure 3a, the Te K-edge XANES spectra for abiological Fe(II)-mediated reduction in the absence of *S. oneidensis* MR-1 present a constant tellurite-like XANES peak feature even in 12 h reaction time, while biological reduction of Te(IV) in the presence of *S. oneidensis* MR-1 surely leads to more distinct metallic tellurium-like XANES feature with increasing incubation time. In the radial distribution function of EXAFS spectra in Figure 3b, the biological reduction of Te(IV) in the presence of *S. oneidensis* MR-1 presents an abrupt decrease of Fourier-transformed (FT) peak for chemical bonding Te(IV)−O at ∼1.45 Å with respect to incubation time, and a distinct development of Fourier-transformed (FT) peak at ∼2.6 Å corresponding to metallic Te−Te interaction. In contrast, the abiological reduction of Te(IV) by Fe(II) shows a constant Te(IV)−O bonding and no FT peak of metallic bonding Te−Te, regardless of chemical reaction time. The suggests that the toxic Te(IV) ion cannot be effectively reduced by the chemical reducing Fe(II) ion itself, although the Fe(II) is able to promote the precipitation of solid tellurite ($Te(IV)O_x$) complex from the Te(IV) solution. Therefore, the existence of *S. oneidensis* MR-1 is certainly necessary to reduce the tellurite (Te(IV)) to metallic tellurium (Te(0)) state. The biological reduction of Te(IV) in the presence of *S. oneidensis* MR-1 started to shows only the FT peak of Te(0)−O bonding in 1h incubation, underwent to evolve the FT peak of the metallic bonding Te−Te from 3h incubation, and

dx.doi.org/10.1021/es401302w | *Environ. Sci. Technol.* 2013, 47, 8709−8715

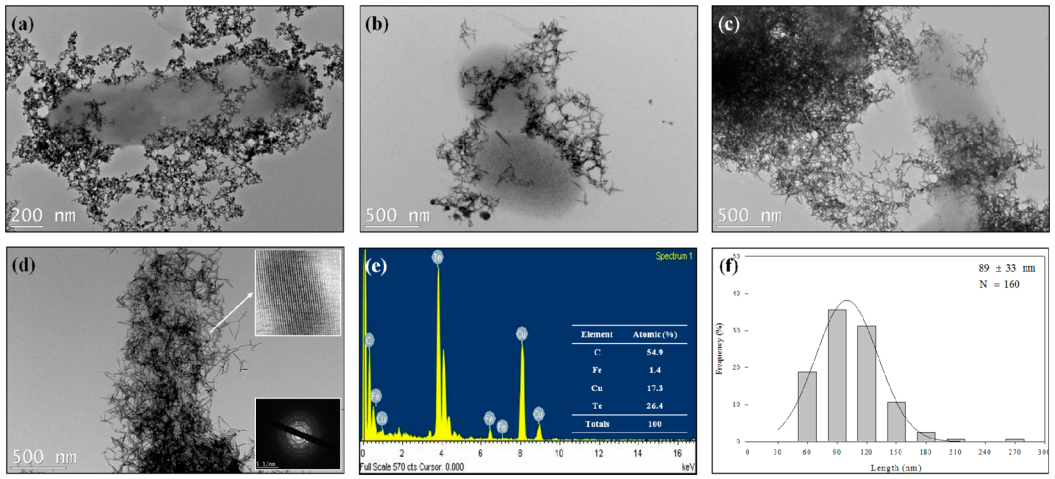

Figure 5. TEM images of (a) to (d) for extracellular Te(0) nanorods formed by preformed Fe(II) with Te(IV) in the presence of *S. oneidensis* MR-1 for 24 h with SAED pattern (d inserted), EDS spectra (e), and length distribution (f) at 24 h incubation. The TEM images of (a) to (d) were taken at 1, 3, 12, and 24 h incubation, respectively.

terminated the formation of metallic FT peak in 12 h (Figure 3b). These results demonstrate that the Te(IV) in a biological medium is not immediately reduced at the moment of initial reaction but rather reduction effectively begins after 3 h incubation. The spectroscopic result suggested that *S. oneidensis* MR-1 in the biological reduction reaction leads to initial reduction of Fe(III) to Fe(II) in the solution followed by the precipitation of tellurite ($Te(IV)O_x$), which likely further reduce to less harmful metallic Te(0) through biological respiration by *S. oneidensis* MR-1. Therefore, considering abundance of iron as a resource in the environments, a concerted biogeochemical reaction between iron reducing bacteria and iron could contribute to effectively alter toxic metal species like Cr(VI), Tc(VII), and CCl_4 with reducing toxicity.[12−19,35,36]

Morphological Analyses of Elemental Tellurium Nanostructures Formed by Various Incubation Conditions. During the incubation of *S. oneidensis* MR-1 in the presence of both Fe(III) and Te(IV) together, the color of incubation medium changed to black, followed by precipitation of the black particles. In contrast, color change and precipitation were not observed in the control experiments lacking either Fe(III) or active *S. oneidensis* MR-1 cells. In addition, direct bacterial Te(IV) reduction by *S. oneidensis* MR-1 in the absence of either Fe(III) or Fe(II) also displayed a blackening, leading to the mostly intracellular and/or surface accumulation of Te(0) nanorods.[9,25] However, TEM images showed that *S. oneidensis* MR-1 in the presence of both Fe(III) and Te(IV) together abundantly accumulated extracellular Te(0) nanostructures (Figure 4). With the incubation time, Fe and Te were initially aggregated around the bacterial cells at 1 h incubation (Figure 4a), followed by formation of the needle-shaped Te(0) nanorods at 3 h incubation (Figure 4b). The Te(0) nanorod structures accumulated continuously on the bacterial cell surfaces over time in incubation (Figure 4c, d). The selected area electron diffraction (SAED) patterns revealed that the Te(0) nanorods were well crystallized structures (Figure 4d inserted). The Te(0) nanorod structures determined by energy-dispersive X-ray spectroscopy (EDS) analysis were composed of 97% of Te and 3% of Fe (Figure 4e). The length and width of the Te(0) nanorods determined by measuring the 120 nanorods were in the range of 240 and 25 nm, respectively (Figure 4f). In comparison, once *S. oneidensis* MR-1 was preincubated with Fe(III) to produce Fe(II) for 24 h, Te(IV) was added to the bacterial culture. Interestingly, the morphology of the Te(0) nanorod structures was shorter and thinner than that of Te(0) nanorods formed by the bacterial culture in the presence of Fe(III) and Te(IV) together (Figures 4 and 5). TEM images illustrated numerous accumulated extracellular Te(0) nanostructures (Figure 5). Initial Fe and Te aggregates at 1 h incubation (Figure 5a) were transformed into needle-shaped Te(0) nanorods at 3 h (Figure 5b), followed by continuous accumulation of Te(0) nanorods on the bacterial cell surfaces during the period of incubation (Figure 5c, d). The high-resolution TEM (HR-TEM) image and SAED patterns revealed that the Te(0) nanorods formed by preformed Fe(II) with Te(IV) in the presence of *S. oneidensis* MR-1 showed crystallized structures (Figure 5d inserted). The EDS analysis of the Te(0) nanorods illustrates a composition of 97% Te and 3% Fe (Figure 5e). The length and width of the Te(0) nanorods determined by measuring the 160 nanorods were in the range of 89 and 7.5 nm, respectively (Figure 5f). The XAFS study for Te(IV) reduction after the preincubation of Fe(III) in the presence of *S. oneidensis* MR-1 shows a different XANES and EXAFS peak features (Figure S2 of the SI). Unlike in the aforementioned reaction of the concurrent existence of Fe(III), Te(IV), and *S. oneidensis* MR-1 in culture medium, the XANES and the FT peak features for the Te(0) nanorods formed by preformed Fe(II) with Te(IV) in the presence of *S. oneidensis* MR-1 demonstrated the metallic peak characteristics in the initial 1 h biological reduction. This suggests that the Te(IV) ion in the solution of preformed Fe(II) in the presence of *S. oneidensis* MR-1 is immediately reduced in the initial reaction followed by the formation of tellurium metallic Te(0) particles.

The phases of products formed by concurrent incubation of Fe(III) and Te(IV) in the presence of *S. oneidensis* MR-1 (Figure S3a of the SI), preformed Fe(II) with Te(IV) in the presence of *S. oneidensis* MR-1 (Figure S3b of the SI), and abiological Fe(II) with Te(IV) in the absence of *S. oneidensis* MR-1 (Figure S3c of the SI) were identified by X-ray diffraction. All of the diffraction peaks were indexed on a hexagonal structure of tellurium (space group *P*3121 (no. 152), powder diffraction file no. 36-1452). However, abiological Fe(II)-mediated formed Te nanoparticles in the absence of *S.*

dx.doi.org/10.1021/es401302w | *Environ. Sci. Technol.* 2013, 47, 8709−8715

oneidensis MR-1 did not exhibit crystal characteristics (Figure S3c of the SI) which was consistent with the X-ray absorption spectroscopic analyses (Figure 3). These results indicate that Fe(III) or Fe(II)-mediate produced Te nanorods in the presence of *S. oneidensis* MR-1 were a single phase of a well-crystallized elemental Te(0) with hexagonal structure. In addition, preformed Fe(II) with Te(IV) in the presence of heat-killed bacterial cells prepared by boiling and autoclaving each for 20 min, or in the presence of metabolically inactivated bacterial cells treated with adding kanamycin (50 μg/mL) did not produce the rod-shaped Te(0) structures while forming only an aggregation of tellurite (Te(IV)O_x) after 24 h reaction (Figure S4 of the SI). Experiments were also conducted to test the possibility that soluble chemical reductants or redox-active proteins were released by *S. oneidensis* MR-1 during metabolism of lactate that might cause extracellular Te(IV) reduction. These cell-free experiments, filtrates of culture medium after growth of *S. oneidensis* MR-1 with lactate and 10 mM of fumarate, were used to test 1 mM Te(IV) reduction in the anaerobic conditions. There was no Te(IV) reduction observed (Figure S5 of the SI), suggesting Te(IV) reduction was started by Fe(II) produced from Fe(III) in the presence of *S. oneidensis* MR-1. Taken together, the results clearly indicated that bacterial *S. oneidensis* MR-1 plays important roles in the shape formation and crystallization of Te(0) nanorods from precipitates as evidenced by the XANES and EXAFS spectral analyses above. Currently, however, we continue seeking the biochemical mechanism for the formation of Te(0) nanorod structures by *S. oneidensis* MR-1.

In summary, addition of Fe(III) to culture medium containing *S. oneidensis* MR-1 and Te(IV) promoted the reduction of Te(IV) to Te(0) under anaerobic conditions. The rapid reduction of Te(IV) is the result of closely coupled biological and abiological reductive reactions in which Fe(II) produced through the dissimilatory Fe(III) reduction by *S. oneidensis* MR-1 helps strain MR-1 reduces Te(IV) to Te(0). Te K-edge X-ray absorption spectrometric analyses shows that although Fe(II) can precipitate Te(IV) to aggregated tellurite (Te(IV)O_x) particles, it cannot fully reduce to elemental tellurium(Te(0)) in the absence of bacterial cells. Therefore, *S. oneidensis* MR-1 plays an important role in the crystallization and growth of the extracellular tellurite (Te(IV)O_x) aggregates to the Te(0) nanorod structures. Furthermore, depending on the bacterial incubation conditions with Fe(III) and Te(IV), the size of Te(0) nanorod structures could be modulated. Due to the diverse optical and electrical properties of Te(0) nanostructures, intensive research activities using physical and chemical techniques have been utilized in an effort to synthesize the Te(0) nanorods.[1,3,37−44] Therefore, current results may provide a new approach for the preparation of well characterized Te(0) nanorods outside of cells as well as the removal of toxic Te(IV) through the environmentally friendly processes.

■ ASSOCIATED CONTENT

Supporting Information

Kinetics of Te(IV) in the aqueaous phase (Figure S1); normalized Te K-edge XANES and corresponding radial distribution function of k^2-weighted Te K-edge EXAFS) (Figure S2); XRD patterns of Te nanostructures (Figure S3); SEM images of Te nanostructures (Figure S4); and kinetics of Te(IV) in the aqueous phase (Figure S5). This material is available free of charge via the Internet at http://pubs.acs.org.

■ AUTHOR INFORMATION

Corresponding Author

*Phone: +82-62-715-2437; fax: +82-62-715-2434; e-mail: hghur@gist.ac.kr.

Notes

The authors declare no competing financial interest.

■ ACKNOWLEDGMENTS

This work was supported by the National Research Foundation of Korea (NRF: 2012-0008725) grant, Ministry of Education, Science & Technology, Republic of Korea.

■ REFERENCES

(1) Sen, S.; Sharma, M.; Kumar, V.; Muthe, K. P.; Satyam, P. V.; Bhatta, U. M.; Roy, M.; Gaur, N. K.; Gupta, S. K.; Yakhmi, J., VI Chlorine gas sensors using one-dimensional tellurium nanostructures. *Talanta* **2009**, *77* (5), 1567−1572.

(2) Tang, Z.; Zhang, Z.; Wang, Y.; Glotzer, S. C.; Kotov, N. A. Self-assembly of CdTe nanocrystals into free-floating sheets. *Science* **2006**, *314* (5797), 274−278.

(3) Turner, R. J.; Borghese, R.; Zannoni, D. Microbial processing of tellurium as a tool in biotechnology. *Biotechnol. Adv.* **2012**, *30* (5), 954−963.

(4) Wang, X.; Liu, G.; Zhou, J.; Wang, J.; Jin, R.; Lv, H. Quinone-mediated reduction of selenite and tellurite by *Escherichia coli*. *Bioresour. Technol.* **2011**, *102* (3), 3268−3271.

(5) Chasteen, T. G.; Fuentes, D. E.; Tantalean, J. C.; Vasquez, C. C. Tellurite: history, oxidative stress, and molecular mechanisms of resistance. *FEMS Microbiol. Rev.* **2009**, *33* (4), 820−832.

(6) Zannoni, D.; Borsetti, F.; Harrison, J. J.; Turner, R. J. The bacterial response to the chalcogen metalloids Se and Te. *Adv. Microb. Physiol.* **2007**, *53*, 1−71.

(7) Taylor, D. E. Bacterial tellurite resistance. *Trends Microbiol.* **1999**, *7* (3), 111−115.

(8) Baesman, S. M.; Bullen, T. D.; Dewald, J.; Zhang, D.; Curran, S.; Islam, F. S.; Beveridge, T. J.; Oremland, R. S. Formation of tellurium nanocrystals during anaerobic growth of bacteria that use Te oxyanions as respiratory electron acceptors. *Appl. Environ. Microbiol.* **2007**, *73* (7), 2135−2143.

(9) Klonowska, A.; Heulin, T.; Vermeglio, A. Selenite and tellurite reduction by *Shewanella oneidensis*. *Appl. Environ. Microbiol.* **2005**, *71* (9), 5607−5609.

(10) Yurkov, V.; Jappe, J.; Vermeglio, A. Tellurite resistance and reduction by obligately aerobic photosynthetic bacteria. *Appl. Environ. Microbiol.* **1996**, *62* (11), 4195−4198.

(11) Liger, E.; Charlet, L.; Van Cappellen, P. Surface catalysis of uranium(VI) reduction by iron(II). *Geochim. Cosmochim. Acta* **1999**, *63* (19−20), 2939−2955.

(12) Jang, J.-H.; Dempsey, B. A.; Burgos, W. D. Reduction of U(VI) by Fe(II) in the presence of hydrous ferric oxide and hematite: Effects of solid transformation, surface coverage, and humic acid. *Water Res.* **2008**, *42* (8−9), 2269−2277.

(13) Fredrickson, J. K.; Zachara, J. M.; Kennedy, D. W.; Kukkadapu, R. K.; McKinley, J. P.; Heald, S. M.; Liu, C.; Plymale, A. E. Reduction of TcO_4^- by sediment-associated biogenic Fe(II). *Geochim. Cosmochim. Acta* **2004**, *68* (15), 3171−3187.

(14) Wielinga, B.; Mizuba, M. M.; Hansel, C. M.; Fendorf, S. Iron promoted reduction of chromate by dissimilatory iron-reducing bacteria. *Environ. Sci. Technol.* **2000**, *35* (3), 522−527.

(15) Lee, T.; Lim, H.; Lee, Y.; Park, J.-W. Use of waste iron metal for removal of Cr(VI) from water. *Chemosphere* **2003**, *53* (5), 479−485.

(16) Lloyd, J. R.; Sole, V. A.; Van Praagh, C. V. G.; Lovley, D. R. Direct and Fe(II)-mediated reduction of technetium by Fe(III)-reducing bacteria. *Appl. Environ. Microbiol.* **2000**, *66* (9), 3743−3749.

(17) Plymale, A. E.; Fredrickson, J. K.; Zachara, J. M.; Dohnalkova, A. C.; Heald, S. M.; Moore, D. A.; Kennedy, D. W.; Marshall, M. J.; Wang, C.; Resch, C. T.; Nachimuthu, P. Competitive reduction of

pertechnetate ($^{99}TcO_4^-$) by dissimilatory metal reducing bacteria and biogenic Fe(II). *Environ. Sci. Technol.* **2011**, *45* (3), 951−957.
(18) Gerlach, R.; Cunningham, A. B.; Caccavo, F. Dissimilatory iron-reducing bacteria can influence the reduction of carbon tetrachloride by iron metal. *Environ. Sci. Technol.* **2000**, *34* (12), 2461−2464.
(19) Xu, W.; Liu, Y.; Zeng, G.; Li, X.; Tang, C.; Yuan, X. Enhancing effect of iron on chromate reduction by *Cellulomonas flavigena*. *J. Hazard. Mater.* **2005**, *126* (1−3), 17−22.
(20) Lall, R.; Mitchell, J. Metal reduction kinetics in *Shewanella*. *Bioinformatics* **2007**, *23* (20), 2754−2759.
(21) Fredrickson, J. K.; Romine, M. F.; Beliaev, A. S.; Auchtung, J. M.; Driscoll, M. E.; Gardner, T. S.; Nealson, K. H.; Osterman, A. L.; Pinchuk, G.; Reed, J. L.; Rodionov, D. A.; Rodrigues, J. L.; Saffarini, D. A.; Serres, M. H.; Spormann, A. M.; Zhulin, I. B.; Tiedje, J. M. Towards environmental systems biology of *Shewanella*. *Nat. Rev. Microbiol.* **2008**, *6* (8), 592−603.
(22) Shi, L.; Squier, T. C.; Zachara, J. M.; Fredrickson, J. K. Respiration of metal (hydr)oxides by *Shewanella* and *Geobacter*: A key role for multihaem *c*-type cytochromes. *Mol. Microbiol.* **2007**, *65* (1), 12−20.
(23) Beliaev, A. S.; Klingeman, D. M.; Klappenbach, J. A.; Wu, L.; Romine, M. F.; Tiedje, J. M.; Nealson, K. H.; Fredrickson, J. K.; Zhou, J. Global transcriptome analysis of *Shewanella oneidensis* MR-1 exposed to different terminal electron acceptors. *J. Bacteriol.* **2005**, *187* (20), 7138−7145.
(24) Lovley, D. R.; Holmes, D. E.; Nevin, K. P. Dissimilatory Fe(III) and Mn(IV) reduction. *Adv. Microb. Physiol.* **2004**, *49*, 219−286.
(25) Kim, D.-H.; Kanaly, R. A.; Hur, H.-G. Biological accumulation of tellurium nanorod structures via reduction of tellurite by *Shewanella oneidensis* MR-1. *Bioresour. Technol.* **2012**, *125*, 127−131.
(26) Lee, J. H.; Kim, M. G.; Yoo, B.; Myung, N. V.; Maeng, J.; Lee, T.; Dohnalkova, A. C.; Fredrickson, J. K.; Sadowsky, M. J.; Hur, H. G. Biogenic formation of photoactive arsenic-sulfide nanotubes by *Shewanella* sp. strain HN-41. *Proc. Natl. Acad. Sci. U.S.A.* **2007**, *104* (51), 20410−20415.
(27) Lee, J.-H.; Roh, Y.; Kim, K.-W.; Hur, H.-G. Organic acid-dependent iron mineral formation by a newly isolated iron-reducing bacterium, *Shewanella* sp. HN-41. *Geomicrobiol. J.* **2007**, *24* (1), 31−41.
(28) Schwertmann, U.; Cornell, R. M. Akaganéite. In *Iron Oxides in the Laboratory*; Wiley-VCH: Verlag GmbH, 2007; pp 113−119.
(29) Tebo, B. M.; Clement, B. G.; Dick, G. J. Biotransformation of manganese. In: *Manual of Environmental Microbiology*; ASM Press: Washington DC, 2007; pp 1223−1238.
(30) Stookey, L. L. Ferrozine—A new spectrophotometric reagent for iron. *Anal. Chem.* **1970**, *42* (7), 779−781.
(31) Deliyanni, E. A.; Peleka, E. N.; Matis, K. A. Removal of zinc ion from water by sorption onto iron-based nanoadsorbent. *J. Hazard. Mater.* **2007**, *141* (1), 176−84.
(32) Sharma, Y. C.; Srivastava, V.; Singh, V. K.; Kaul, S. N.; Weng, C. H. Nano-adsorbents for the removal of metallic pollutants from water and wastewater. *Environ. Technol.* **2009**, *30* (6), 583−609.
(33) Deliyanni, E. A.; Bakoyannakis, D. N.; Zouboulis, A. I.; Matis, K. A. Sorption of As(V) ions by akaganéite-type nanocrystals. *Chemosphere* **2003**, *50* (1), 155−163.
(34) Lazaridis, N. K.; Bakoyannakis, D. N.; Deliyanni, E. A. Chromium(VI) sorptive removal from aqueous solutions by nanocrystalline akaganèite. *Chemosphere* **2005**, *58* (1), 65−73.
(35) Boland, D. D.; Collins, R. N.; Payne, T. E.; Waite, T. D. Effect of amorphous Fe(III) oxide transformation on the Fe(II)-mediated reduction of U(VI). *Environ. Sci. Technol.* **2011**, *45* (4), 1327−1333.
(36) Cooper, D. C.; Picardal, F.; Rivera, J.; Talbot, C. Zinc immobilization and magnetite formation via ferric oxide reduction by *Shewanella putrefaciens 200*. *Environ. Sci. Technol.* **1999**, *34* (1), 100−106.
(37) Liao, K.-S.; Wang, J.; Dias, S.; Dewald, J.; Alley, N. J.; Baesman, S. M.; Oremland, R. S.; Blau, W. J.; Curran, S. A. Strong nonlinear photonic responses from microbiologically synthesized tellurium nanocomposites. *Chem. Phys. Lett.* **2010**, *484* (4−6), 242−246.
(38) Lloyd, J. R.; Byrne, J. M.; Coker, V. S. Biotechnological synthesis of functional nanomaterials. *Curr. Opin. Biotech.* **2011**, *22* (4), 509−515.
(39) Lu, Q.; Gao, F.; Komarneni, S. Biomolecule-assisted reduction in the synthesis of single-crystalline tellurium nanowires. *Adv. Mater.* **2004**, *16* (18), 1629−1632.
(40) Wang, Z.; Wang, L.; Huang, J.; Wang, H.; Pan, L.; Wei, X. Formation of single-crystal tellurium nanowires and nanotubes via hydrothermal recrystallization and their gas sensing properties at room temperature. *J. Mater. Chem.* **2010**, *20* (12), 2457−2463.
(41) Zhang, B.; Hou, W.; Ye, X.; Fu, S.; Xie, Y. 1D tellurium nanostructures: Photothermally assisted morphology-controlled synthesis and applications in preparing functional nanoscale materials. *Adv. Funct. Mater.* **2007**, *17* (3), 486−492.
(42) Zhu, H.; Zhang, H.; Liang, J.; Rao, G.; Li, J.; Liu, G.; Du, Z.; Fan, H.; Luo, J. Controlled synthesis of tellurium nanostructures from nanotubes to nanorods and nanowires and their template applications. *J. Phys. Chem. C* **2011**, *115* (14), 6375−6380.
(43) Salavati-Niasari, M.; Bazarganipour, M.; Davar, F. Solution-chemical syntheses of nanostructure HgTe via a simple hydrothermal process. *J. Alloy. Compd.* **2010**, *499* (1), 121−125.
(44) Salavati-Niasari, M.; Bazarganipour, M.; Davar, F. Hydrothermal preparation and characterization of based-alloy Bi_2Te_3 nanostructure with different morphology. *J. Alloy. Compd.* **2010**, *489* (2), 530−534.